Adaptive Line Enhancers for Fast Acquisition

H.-G. Yeh
Spacecraft Telecommunications Equipment Section

T. M. Nguyen
Communications Systems Research Section

Three adaptive line enhancer (ALE) algorithms and architectures—namely, conventional ALE, ALE with double filtering, and ALE with coherent accumulation—are investigated for fast carrier acquisition in the time domain. The advantages of these algorithms are their simplicity, flexibility, robustness, and applicability to general situations including the Earth-to-space uplink carrier acquisition and tracking of the spacecraft. In the acquisition mode, these algorithms act as bandpass filters; hence, the carrier-to-noise ratio (CNR) is improved for fast acquisition. In the tracking mode, these algorithms simply act as lowpass filters to improve signal-to-noise ratio; hence, better tracking performance is obtained. It is not necessary to have a priori knowledge of the received signal parameters, such as CNR, Doppler, and carrier sweeping rate. The implementation of these algorithms is in the time domain (as opposed to the frequency domain, such as the fast Fourier transform (FFT)). The carrier frequency estimation can be updated in real time at each time sample (as opposed to the batch processing of the FFT). The carrier frequency to be acquired can be time varying, and the noise can be non-Gaussian, nonstationary, and colored.

I. Introduction

The present spacecraft transponder acquires and tracks the carrier signal by using a phase-locked loop (PLL). Because the frequency sweeping technique is employed in the acquisition process, the time that it takes for the PLL to acquire the uplink carrier is relatively long. The sweeping rate is set to about 40 Hz/sec when the spacecraft receiver signal-to-noise ratio (SNR) equals −151 dBm for a deep-space mission. To sweep ±10 kHz from the best locked frequency, 17 min are required to complete the acquisition process. Therefore, there is a need for fast-acquisition technique development with application to the transponder. In general, a fast-acquisition technique as shown in Fig. 1 will be very useful for deep-space missions, especially in emergencies. First, the receiver is in the acquisition process. Second, when the uplink carrier is acquired and indicated by the lock detector, the switch is then shifted to the tracking position and the tracking process takes over immediately. Although devised to support the space mission, the fast-acquisition technique proposed in this article is also applicable to other types of receivers, including fixed-ground and mobile receivers.

The problem of estimating certain parameters of a sinusoidal signal in the presence of noise is of general interest and has received considerable attention in the literature [1]. Examples may be found in vibration measurements, Doppler radar returns, geophysical processing, and communication systems [2].

Many techniques, such as the fast Fourier transform (FFT) [3] and adaptive least-squares algorithms [4], have been proposed in the literature to solve such problems. These methods provide excellent results but may require excessively long observation times because of batch processing.

Recently, time-domain spectral estimation techniques based on an adaptive line enhancer (ALE) system have been introduced [5-9]. The ALE system is depicted in Fig. 2. The system, which was introduced by

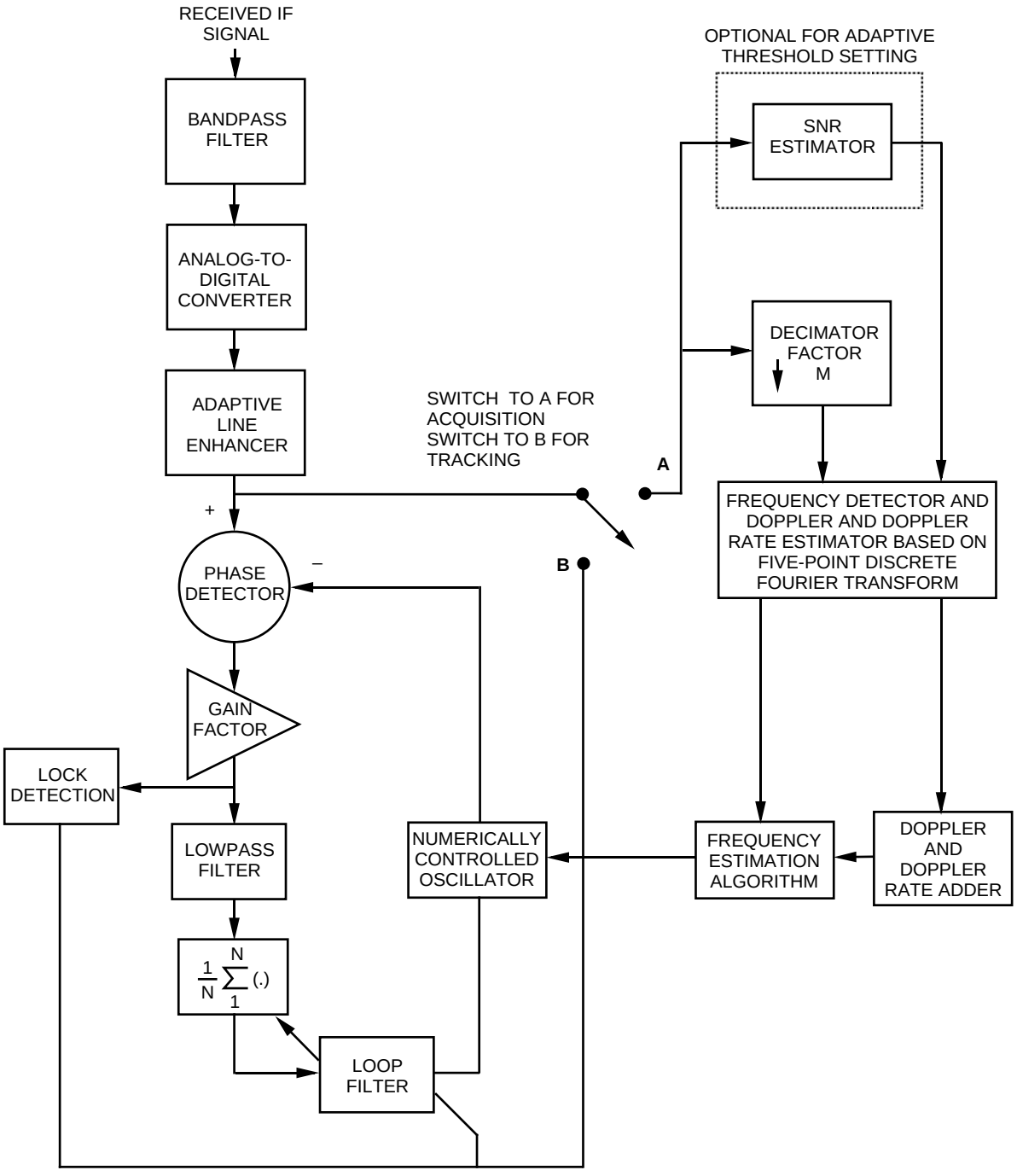

Fig. 1. Using ALE in the digital receiver for both acqusition and tracking.

Widrow [5], uses the measured signal as the desired response and a delayed version of itself as input. The principle is that the delay should decorrelate the noise between the primary and reference inputs while leaving the narrowband carrier signal correlated. When functioning ideally, the adaptive filter output is an enhanced version of the carrier components with a higher carrier-to-noise ratio (CNR). Both CNR and SNR are used in this article, and they are interchangeable.

The adaptive filter depicted in Fig. 2 is a time-varying system and the weight vector is updated, based on the least-mean-squares (LMS) algorithm. The LMS algorithm is based on the method of steepest descent [5]. Many applications have been developed using the LMS algorithm; the fast measurement of digital instantaneous frequency in [6] and [12] are examples. In addition, it is well known that the LMS-type algorithms are more robust to sudden variations in the environment than the FFT algorithms.

Three ALE algorithms and architectures for fast acquisition are presented in this article. The analysis of the general properties of an ALE is given in Section II. It contains discussion of an optimal adaptive filter, optimal gain, and a steady-state frequency response. Section III introduces two modified ALE algorithms: the ALE with double filtering (ALEDF) and the ALE with coherent accumulation (ALECA). Implementation is considered in Section IV. Simulations for acquiring fixed-frequency-signal acquisition are provided in Section V. Performance comparison of these adaptive line enhancers is also discussed in Section V. A discussion and the conclusion are given in Section VI.

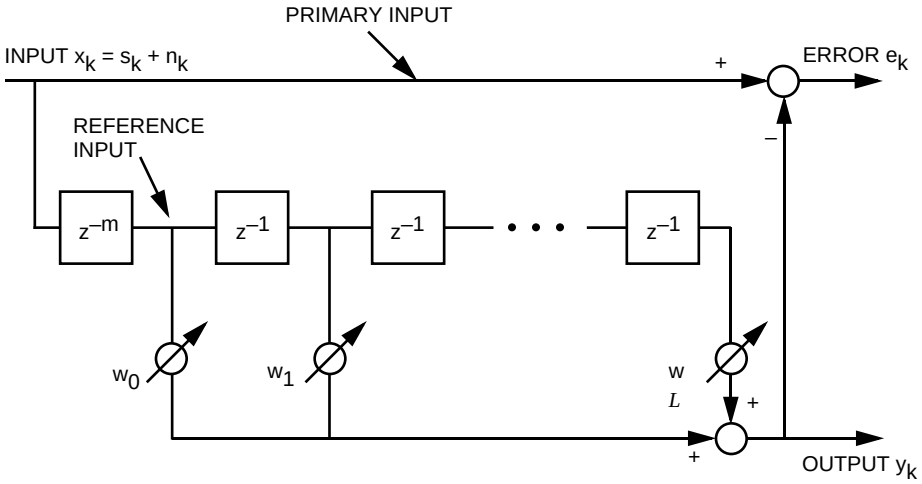

Fig. 2. The structure of the conventional adaptive line enhancer.

II. Analysis of the Optimal ALE

It is shown in [10] that, in general, the real LMS algorithm is not equivalent to the real part of the complex LMS algorithm. However, when the algorithm is configured as an ALE with sinusoidal inputs, the mean weight behavior of the real algorithm is identical to the real part of the mean weight of the complex algorithm. There are simplicities in the analysis of the complex model that do not exist in the analysis of the real model. Consequently, the analysis will be performed by using complex models in Sections II and III. Both the system gain and the steady-state frequency response of the ALE are provided in this section.

A. The Optimal Adaptive Filter

The input signal of Fig. 2 is x_k, which contains carrier component s_k and white noise component n_k with power σ_n^2. The signal at the primary input is defined as

$$\begin{aligned} x_k &= s_k + n_k \\ &= ae^{j(\omega_o kT+\phi)} + n_k \end{aligned} \tag{1}$$

where a denotes the signal amplitude, ϕ denotes the signal phase, T is the sampling period, and ω_o is the carrier frequency.

In vector/matrix form,

$$\begin{aligned} \mathbf{x}_k &= \mathbf{s}_k + \mathbf{n}_k \\ &= ae^{j(\omega_o kT+\phi)}\mathbf{q} + \mathbf{n}_k \end{aligned} \tag{2}$$

where

$$\mathbf{x}_k = [x_k \;\; x_{k-1} \;\; \cdots \;\; x_{k-L}]^T \tag{3}$$

$$\mathbf{q} = \left[1 \;\; e^{-j\omega_o T} \;\; e^{-j2\omega_o T} \;\; \cdots \;\; e^{-jL\omega_o T}\right]^T \tag{4a}$$

$$\mathbf{n}_k = [n_k \;\; n_{k-1} \;\; \cdots \;\; n_{k-L}]^T \tag{4b}$$

are vectors of length $(L+1)$. The input signal vector to the adaptive filter is $\mathbf{x}_{k-m}$, where m is the delay unit. The delay unit m chosen must be of sufficient length to cause the broadband noise components in the filter (reference) input to become uncorrelated from those in the primary input. The carrier signal components, because of their periodic nature, will remain correlated with each other. The adaptive filter output is

$$y_k = \mathbf{w}_k^h \mathbf{x}_{k-m} \tag{5}$$

where $\mathbf{w}_k = [w_0 \; w_1 \; \cdots \; w_L]^T$ and H denotes the conjugate transpose. The error sequence is defined as

$$e_k = x_k - y_k \tag{6}$$

The weight vector is updated as follows:

$$\mathbf{w}_{k+1} = \mathbf{w}_k + 2\mu e_k \mathbf{x}_{k-m}^* \tag{7}$$

where * denotes the conjugate operation and μ is the step size of the adaptation.

The convergence of the weight vector is assured by [5]

$$O < \mu < \frac{1}{(L+1)(carrier + noise\ power)} \tag{8}$$

where $L+1$ is the number of taps of the adaptive filter. The optimal weight vector w_{opt}, called the Wiener weight vector, is found in [5] as

$$\mathbf{w}_{opt} = \mathbf{R}^{-1}\mathbf{p} \tag{9}$$

where

$$\mathbf{R} = E\left[\mathbf{x}_{k-m}\mathbf{x}_{k-m}^{H}\right] = \mathbf{R}_s + \mathbf{R}_N = a^2\mathbf{q}\mathbf{q}^H + \sigma_n^2\mathbf{I} \tag{10}$$

$$\mathbf{R}_s = \text{autocorrelation matrix of the carrier}$$

$$\mathbf{R}_n = \text{autocorrelation matrix of the noise with power } \sigma_n^2$$

$$\mathbf{p} = E\left[\mathbf{x}_{k-m}\mathbf{x}_k^*\right] = a^2 e^{-j\omega_o mT}\mathbf{q} \tag{11}$$

By applying the matrix inversion lemma, also called the "**ABCD** lemma,"

$$(\mathbf{A}+\mathbf{BCD})^{-1} = \mathbf{A}^{-1}[\mathbf{I}-\mathbf{B}(\mathbf{DA}^{-1}\mathbf{B}+\mathbf{C}^{-1})^{-1}\mathbf{DA}^{-1}] \tag{12}$$

The $\mathbf{R}^{-1}$ is obtained as follows:

$$\mathbf{R}^{-1} = \left(\sigma_n^2\mathbf{I} + a^2\mathbf{q}\mathbf{I}\mathbf{q}^H\right)^{-1} = \frac{1}{\sigma_n^2}\left[\mathbf{I} - \frac{a^2}{\sigma_n^2 I + (L+1)a^2}\mathbf{q}\mathbf{q}^H\right] \tag{13}$$

where

$$\mathbf{A} = \sigma_n^2\mathbf{I} \tag{14}$$

$$\mathbf{B} = a^2\mathbf{q} \tag{15}$$

$$\mathbf{C} = \mathbf{I} \tag{16}$$

$$\mathbf{D} = \mathbf{q}^H \tag{17}$$

The optimal weight is then obtained as follows:

$$\mathbf{w}_{opt} = \mathbf{R}^{-1}\mathbf{p} = \beta z_0^{-m}\mathbf{q} \tag{18}$$

where

$$\beta = \frac{a^2}{\sigma_n^2 + (L+1)a^2} \tag{19}$$

$$z_0 = e^{j\omega_o T} \tag{20}$$

When the adaptive filter converges to its steady state, the weight vector fluctuates around its optimal solution.

B. The Optimal Coherent Processing Gain of the ALE

The optimal linear solution for selecting the weight vector of an ALE is similar to that for the so-called "matched filter." For a carrier at frequency ω_o embedded in white noise, the matched filter response is a sampled sinusoidal signal whose frequency is ω_o. The matched filter produces the peak SNR at each sample, but does not preserve the carrier signal waveform at the output, especially when the input signal has time-varying parameters. The matched filter solution does provide the best SNR gain obtainable by linear processing. However, the solution can be constructed only by giving prior knowledge of the frequency ω_o. On the other hand, the ALE output y_k preserves the carrier signal waveform as shown in Eq. (21). Furthermore, it is not necessary to have a priori knowledge of the received signal parameters, such as carrier SNR, Doppler, and carrier sweeping rate. For example, the carrier frequency sweeping rate depends on the uplink carrier signal level for a deep-space mission. The uplink carrier frequency ω_o sweeping rate is set to about 544 and 40 Hz/sec around the best-lock frequency when the carrier signal level is equal to -110 and -151 dBm, respectively. Therefore, the ALE method is designed to approximate the optimal SNR gain obtained by the matched filter solution for this problem.

The optimal steady-state carrier component at the ALE system output is

$$y_{sk} = \mathbf{w}_{opt}^H \mathbf{x}_{k-m} = gae^{j(\omega_o kT+\phi)} = gs_k \tag{21}$$

where the optimal coherent processing gain is

$$g = \frac{(L+1)a^2}{(L+1)a^2+\sigma_n^2} = (L+1)\beta \tag{22}$$

Clearly, the carrier component at the ALE output has the same phase (or delayed by $2\pi n, n$ being an integer) as the input signal and is multiplied by the real processing gain factor g. The ALE system total power output at steady state is

$$E\left[y_k y_k^*\right] = E\left\{\left[\mathbf{w}_{opt}^H \mathbf{x}_{k-m}\right]\left[\mathbf{w}_{opt}^H \mathbf{x}_{k-m}\right]^H\right\} = \mathbf{w}_{opt}^H \mathbf{R}\mathbf{w}_{opt} \tag{23}$$

Substituting Eqs. (10) and (18) into Eq. (23), the ALE system total power output becomes

$$E\left[y_k y_k^*\right] = g^2\left[a^2 + \frac{\sigma_n^2}{L+1}\right] \tag{24}$$

This ALE system output CNR is then obtained as follows:

$$\mathbf{CNR}_{out} = \frac{output\ carrier\ power}{output\ noise\ power} = \frac{E[y_s^2(k)]}{E[y_n^2(k)]} = \frac{(L+1)a^2}{\sigma_n^2} \tag{25}$$

The ALE system input CNR power ratio is

$$\mathbf{CNR}_{input} = \frac{input\ carrier\ power}{input\ noise\ power} = \frac{a^2}{\sigma_n^2} \tag{26}$$

Therefore, the ALE optimal steady-state CNR gain is

$$\mathbf{G_{ALE}} = \frac{\mathbf{CNR}_{output}}{\mathbf{CNR}_{input}} = L + 1 \tag{27}$$

Equation (27) shows that the ALE optimal CNR gain is proportional to the length of the adaptive filter.

C. The Steady-State Frequency Response of the Optimal ALE

From Fig. 2 and using the z-transform, one can derive the transfer function of the ALE. It is obtained as follows:

$$\mathbf{H}(z) = \frac{\mathbf{Y}(z)}{\mathbf{X}(z)} = z^{-m}\mathbf{W}(z) \tag{28}$$

where

$$\mathbf{W}(z) = \mathbf{Z}\left\{\mathbf{w}^*_{opt}(k)\right\} = \beta z_0^m \sum_{i=0}^{L} z_0^i z^{-i} = \beta z_0^m \frac{1-(z_0 z^{-1})^{(L+1)}}{1 - z_0 z^{-1}} \tag{29}$$

Therefore, $\mathbf{H}(z)$ is

$$\mathbf{H}(z) = \beta z^{-m} z_0^m \frac{1-(z_0 z^{-1})^{(L+1)}}{1 - z_0 z^{-1}} \tag{30}$$

Consequently, the optimal steady-state frequency response of the ALE is

$$\begin{aligned} \mathbf{H}(\omega) &= \beta e^{j(\omega_o-\omega)mT} \frac{1 - e^{j(\omega_o-\omega)T(L+1)}}{1 - e^{j(\omega_o-\omega)T}} \\ &= \beta e^{j(\omega_o-\omega)(m+L/2)T} \frac{\sin\left[((L+1)/2)(\omega_o-\omega)T\right]}{\sin\left[(1/2)(\omega_o-\omega)T\right]} \end{aligned} \tag{31}$$

At $\omega = \omega_o$, the optimal frequency response (the peak value of the transfer function) becomes

$$\mathbf{H}(\omega_o) = \beta(L+1) = g \tag{32}$$

Equation (32) shows a real constant gain g at the frequency ω_o, which is the acquired or tracked carrier frequency.

Steady-state magnitude responses of the optimal ALE with filter lengths of 16- and 32-taps are shown in Fig. 3, where the sampling frequency is equal to $10\omega_o$. It is observed that the magnitude response of the 32-tap ALE has much sharper cutoff frequency and twice the frequency resolution of the 16-tap ALE. It also shows that the ALE acts as a bandpass filter and the center frequency of the ALE is adapted to track the frequency of the input carrier signal. Consequently, when the ω_o of the input carrier is changed (either increased or decreased), the center frequency of the bandpass filter will follow. Furthermore, the

steady-state response of the ALE at frequency ω_o is related to the input CNR and the length of the weight as depicted in Eq. (33):

$$20\ \log|\mathbf{H}(\omega_o)| = 20\ \log(g) = 20\ \log\frac{(L+1)\mathbf{CNR}_{input}}{1+(L+1)\mathbf{CNR}_{input}}\ \text{dB} \tag{33}$$

Equation (33) is plotted and shown in Fig. 4. It shows that, at high input CNR, the adaptive filter has a gain close to 1. This means that the carrier will pass through the adaptive filter (filter weighting function is about 1) nearly 100 percent; the error sequence obtained after the subtraction is minimized in the least-mean-square sense. At low input carrier SNR (SNR < -20 dB), the adaptive filter gain is close to 0. This indicates that when the noise component is much stronger than the carrier component, the best filter gain obtained should be small so that the error sequence will not increase in the least-square sense.

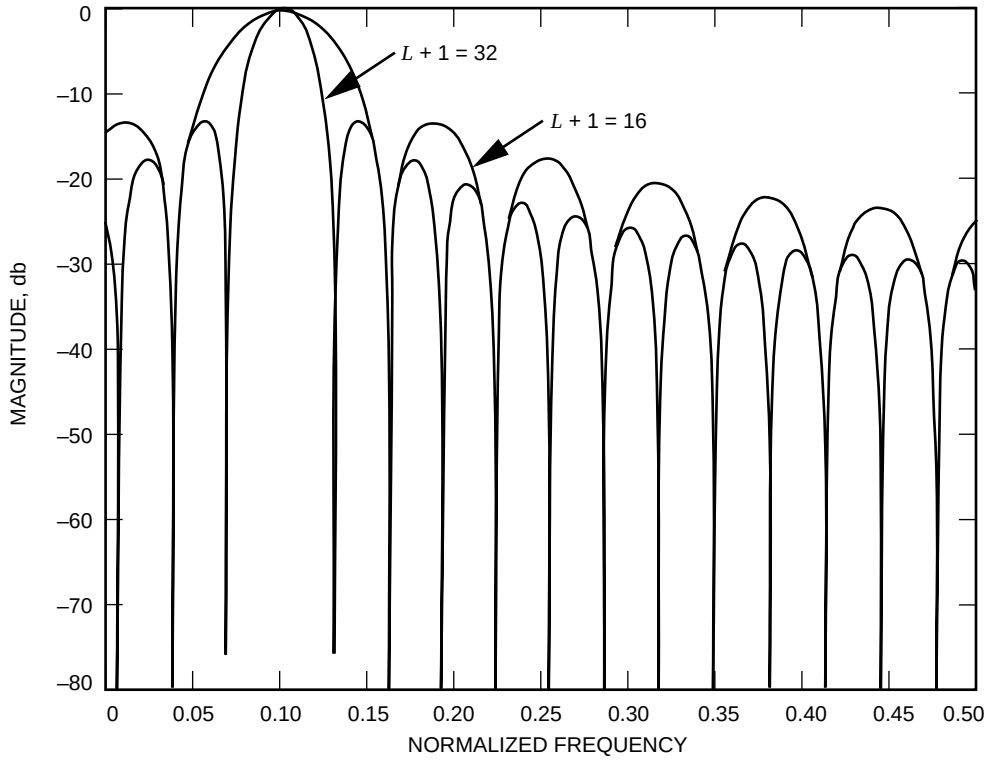

Fig. 3. The magnitude response of the optimal ALE with filter lengths of 16 and 32.

III. The ALEDF and ALECA Algorithms

In general, the ALE's CNR gain can be doubled by doubling the length based on Eq. (27), which also doubles the frequency resolution. However, this means that the total number of operations required will be doubled. Two ALEs, modified to improve the ALE system performance at the given frequency resolution and without increasing the computational load too much, are presented in this section.

A. The Adaptive Line Enhancer With Double Filtering

The first modified ALE is the so-called ALE with double filtering (ALEDF) and is shown in Fig. 5. A finite-impulse response (FIR) filter is cascaded with the ALE as the second stage. Coefficients of this FIR

filter are a real-time copy of those of the adaptive filter in the ALE. By filtering the received signal using two identical filters, the overall system gain is squared in linear scale or doubled in dB scale. Consequently, the overall processing gain at the desired signal of the ALEDF is equal to g^2. However, the processing time of this ALEDF is $2(L+1)T$, where T is the sampling period. Note that the processing time of an ALE with $2(L+1)$ taps is the same as that of the ALEDF with $(L+1)$ taps per filter. The magnitude responses of both the ALEDF and ALE with 16 taps per filter are given in Fig. 6. Both magnitude responses have the same frequency resolution. Due to double filtering, the magnitude response of the ALEDF has a sharper cutoff frequency and much lower sidelobes compared with those of the ALE, as shown in Fig. 6. However, the magnitude response of the ALEDF of Fig. 6 has half-frequency resolution and much lower sidelobes compared with those of the ALE with 32 taps, as shown in Fig. 3. This is due to the fact that the ALEDF has two 16-tap filters in cascade while the ALE has 32-tap filters.

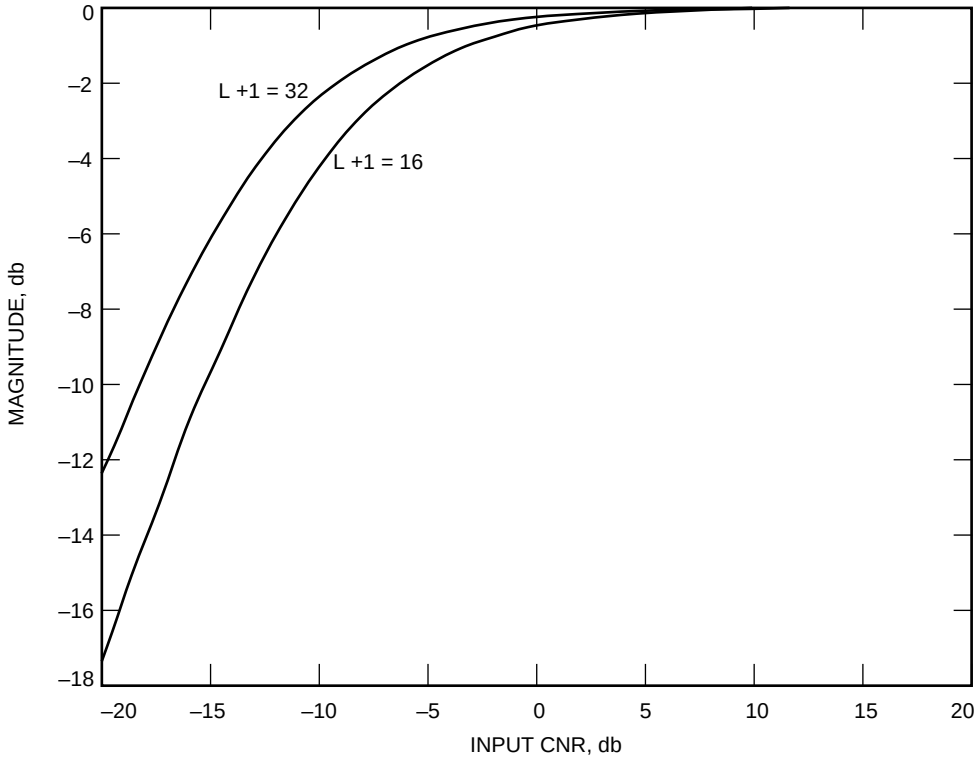

Fig. 4. The coherent processing gain magnitude response of the optimal ALE at the tracked frequency ω_o versus the input CNR.

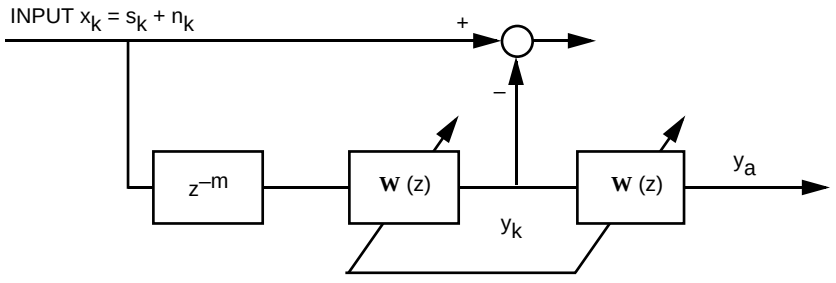

Fig. 5. The structure of the adaptive line enhancer with double filtering (ALEDF).

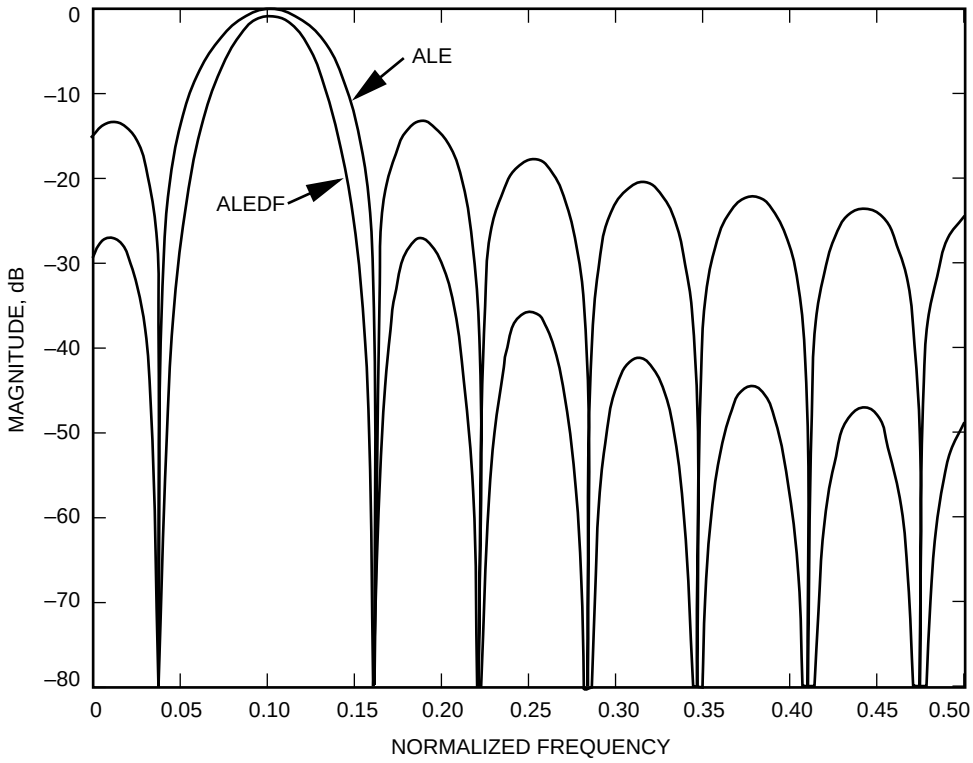

Fig. 6. The optimal magnitude response of both the ALEDF and ALE; filter length = 16.

B. The Adaptive Line Enhancer With Coherent Accumulation

The second modified architecture is the so-called ALE with coherent accumulation (ALECA); it is depicted in Fig. 7. The ALECA was first introduced in [11]. Figure 7 shows that an ALE output is cascaded with a closed feedback loop. This loop contains real-time copied filter coefficients from the adaptive filter of the ALE, an m-delay unit, and a multiplication parameter c. The output of the ALE is the input of the second stage. It has been shown in Eq. (21) that the carrier component of the ALE output y_k has the same phase as the input carrier component. By applying the same processing in the feedback loop (i.e., the same delay units and same filter as that of the reference input line in the ALE), the carrier component of y_b will have the same phase as that of y_k. Therefore, it is an ALE with coherent accumulation to produce the final output y_a.

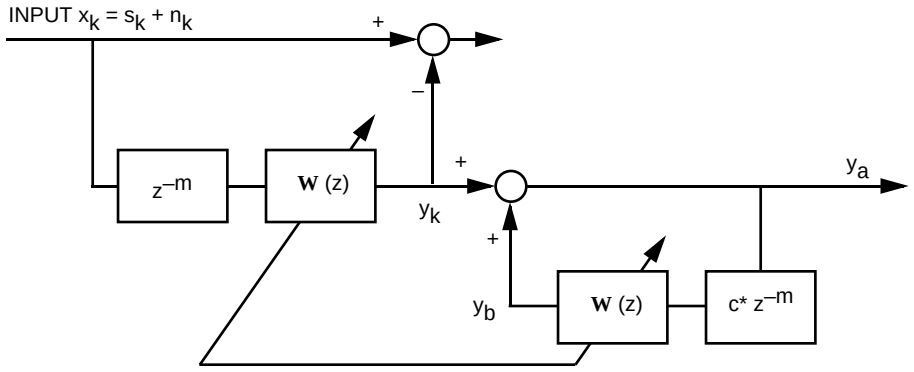

Fig. 7. The structure of the adaptive line enhancer with coherent accumulation (ALECA).

This ALECA architecture uses a recursive loop. Consequently, the stability of the system is of concern. To ensure the stability of the ALECA system, the feedback parameter c must be less than 1 and greater than or equal to 0 (Appendix). The ALECA becomes a conventional ALE when $c = 0$. The ALECA system performance is analyzed and given in the following sections.

1. The Steady-State Frequency Response of the Optimal ALECA. From Fig. 7, the overall transfer function is

$$\mathbf{H}_a(z) = \frac{\mathbf{Y}_a(z)}{\mathbf{X}(z)} = \frac{\mathbf{H}(z)}{1 - c\mathbf{H}(z)} \tag{34}$$

Therefore, the steady-state frequency response to the input s_k is

$$\mathbf{H}_a(\omega) = \frac{\beta e^{j(\omega_o-\omega)(m+L/2)T} \frac{\sin[((L+1)/2)(\omega_o-\omega)T]}{\sin[(1/2)(\omega_o-\omega)T]}}{1 - c\beta e^{j(\omega_o-\omega)(m+L/2)T} \frac{\sin[((L+1)/2)(\omega_o-\omega)T]}{\sin[(1/2)(\omega_o-\omega)T]}} \tag{35}$$

At $\omega = \omega_o$, the frequency response becomes

$$\mathbf{H}_a(\omega_o) = \frac{g}{1 - cg} \tag{36}$$

Note that g is less than or equal to 1. When c approaches $1/g, \mathbf{H}_a(\omega_o)$ becomes infinite. Consequently, the magnitude response at $\omega = \omega_o$ versus input CNR is obtained and given in Eq. (37):

$$20\ \log|\mathbf{H}_a(\omega_o)| = 20\ \log|\frac{g}{1-cg}| = 20\ \log|\frac{(L+1)\mathbf{CNR}_{input}/(1+(L+1)\mathbf{CNR}_{input})}{1 - c\,[(L+1)\mathbf{CNR}_{input}/(1+(L+1)\mathbf{CNR}_{input})]}\ \text{dB} \tag{37}$$

2. ALECA System Performance. Figure 8 shows the magnitude response of the optimal ALECA at $\omega = \omega_o$ versus input CNR based on Eq. (37). Figure 9 shows the magnitude response of the optimal ALECA versus the frequency based on Eq. (35) with several different c values. When parameter c equals zero, the ALECA becomes the conventional ALE. When parameter c is close to 1, the peak value of the ALECA transfer function is significantly higher than that of the conventional ALE, which also leads to some improvement in CNR gain due to the smaller effective noise bandwidth.

IV. Implementation Considerations

Starting with this section, only the real (not complex) case is considered. The total number of operations required is $2L+2$ for both multiplications and accumulations of an ALE system using Eqs. (15) and (17) with a filter length of $L+1$. However, the computation of the ALEDF with $L+1$ taps would require $3L+3$ multiplications and $3L+2$ additions. This is because Eq. (17) is employed once while Eq. (15) is used twice. The total number of multiplications and additions required of an ALE with $2(L+1)$ taps is $4L+4$ and $4L+4$, respectively. However, this $(2L+2)$-tap ALE has twice the frequency resolution and CNR gain of the $2(L+1)$-tap ALE. Clearly, 25 percent of the multiplications and additions are saved in the ALEDF with $L+1$ taps in comparison with $2(L+1)$-tap ALE. The total number of multiplications and accumulations required of the ALECA with the filter length of $L+1$ is $3L+4$ and $3L+3$, respectively. Table 1 shows the computational load comparison between several ALE architectures.

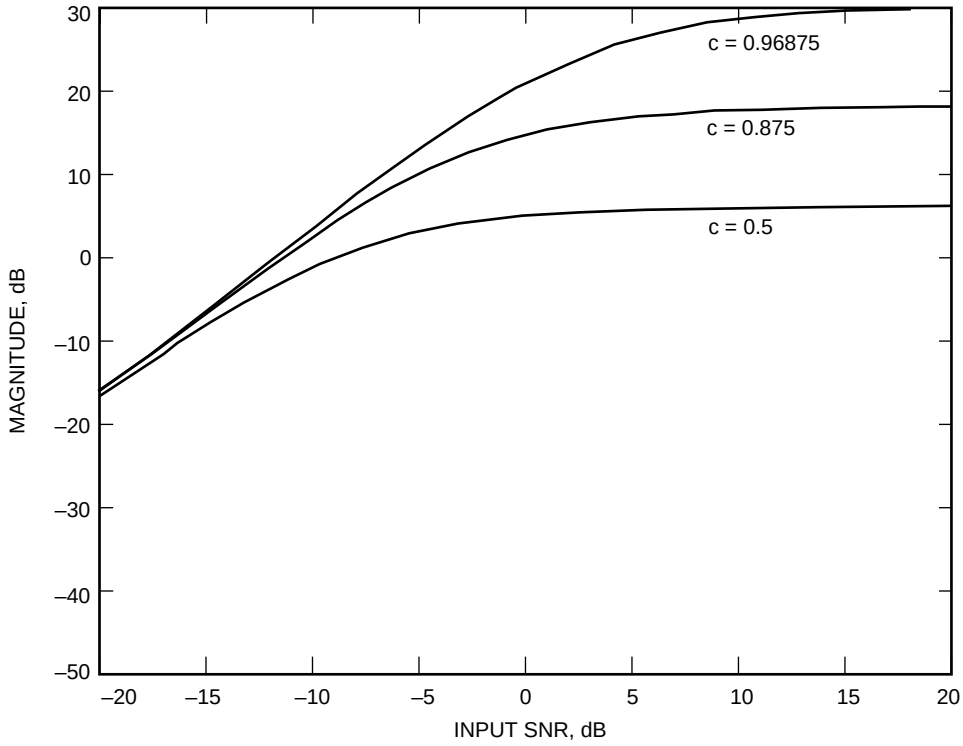

Fig. 8. The magnitude response of the optimal ALECA at $\omega = \omega_o$ versus the input CNR.

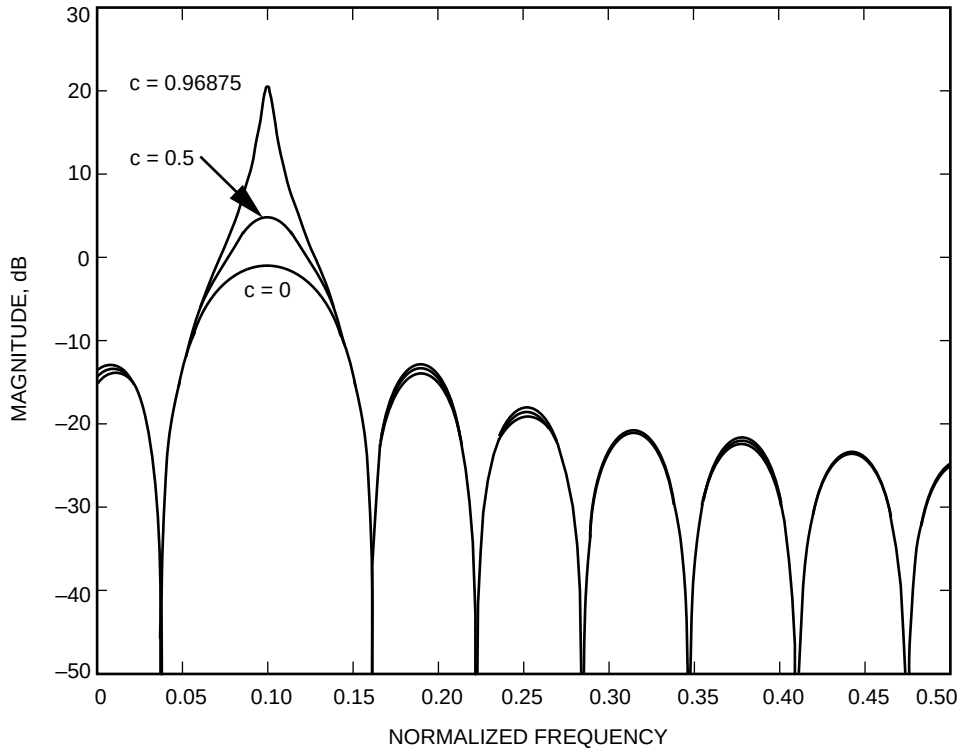

Fig. 9. The magnitude response of the optimal ALECA versus the frequency.

Table 1. The computational load comparison between several ALE architectures.

Number of operations	ALE (filter length: $L+1$)	ALEDF (length: $L+1$/filter)	ALECA (length: $L+1$/filter)
Multiplications	$2L\ +\ 2$	$3L\ +\ 3$	$3L\ +\ 4$
Additions	$2L\ +\ 2$	$3L\ +\ 2$	$3L\ +\ 3$

V. Simulations

The tracking performances of the 16-tap ALE, ALEDF, and ALECA are studied via simulations with the same frequency resolution for comparison. The carrier is a sinusoidal signal with a fixed frequency, and the sampling rate is 256 times the carrier frequency. Figure 10 shows the input signal in the time domain with SNR = 0 dB. Figures 11, 12, and 13 present the carrier estimation obtained by the ALE, ALEDF, and ALECA, respectively. The total number of weights is 16 per filter, the number of delays is chosen as 1, and the parameter c is equal to 0.96875. The step size chosen is 0.000625. Visual examination indicates that the ALECA output provides the best estimated carrier signal, the ALEDF output is second, and the conventional ALE is last. To show the frequency response of the filtered sequence, the sampling frequency is changed to eight times the carrier frequency for better resolution. All other conditions are the same as the time-domain simulation.

Figures 14 through 17 show the frequency-domain response of the input sequence, the ALE output data, the ALEDF output data, and the ALECA output data, respectively. The location of the simulated carrier frequency is indicated on Figs. 14 through 16 by vertical arrows on the x-axis. The desired signal gain of the ALECA is greater than that of either the ALE or the ALEDF.

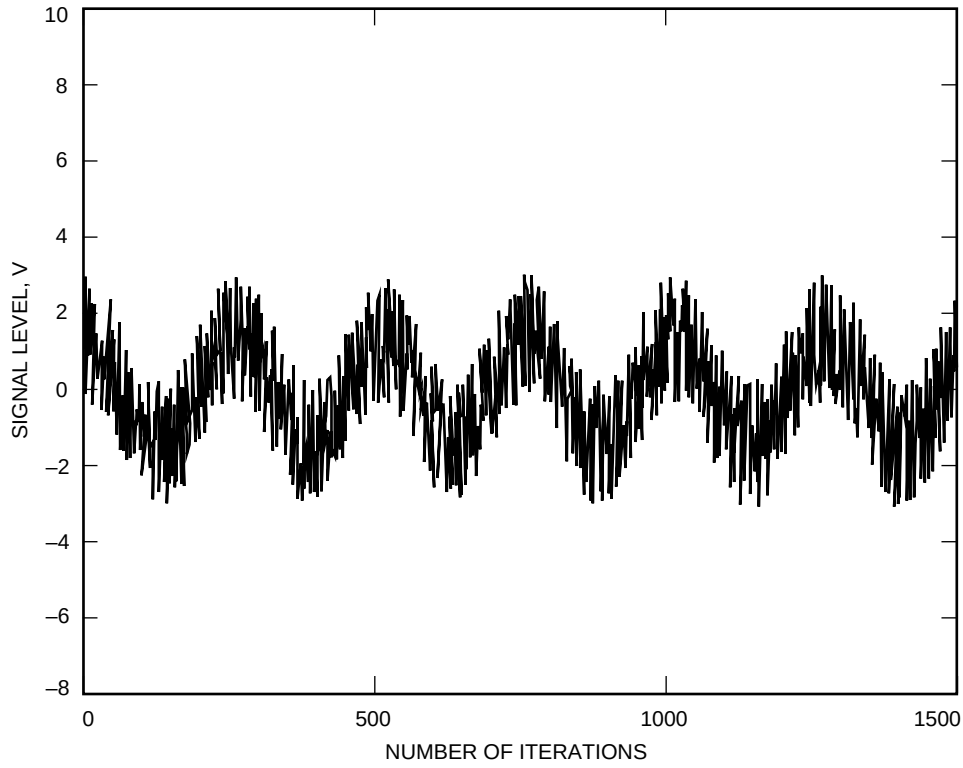

Fig. 10. The ALE input signal in time domain with SNR = 0 dB.

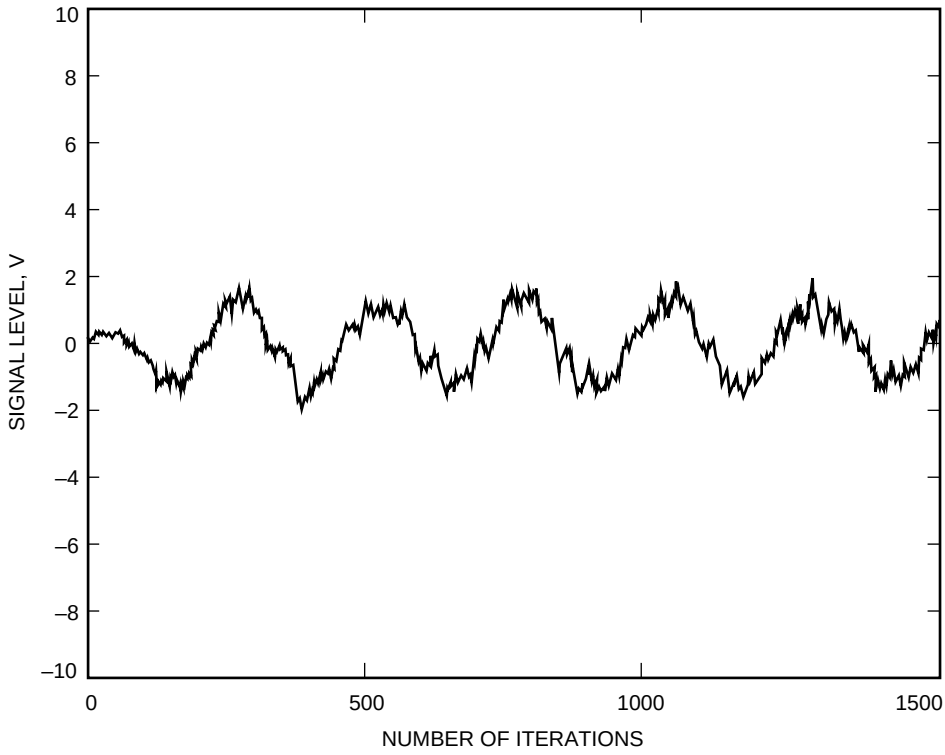

Fig. 11. The 16-tap ALE output: an estimated carrier signal.

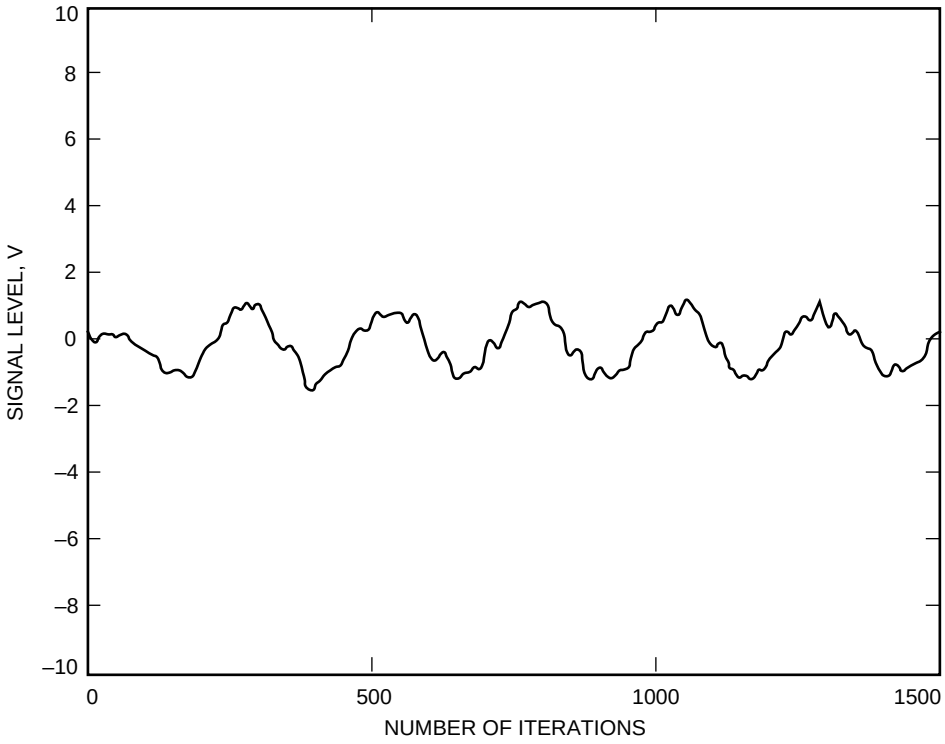

Fig. 12. The 16-tap ALEDF output: an estimated carrier signal.

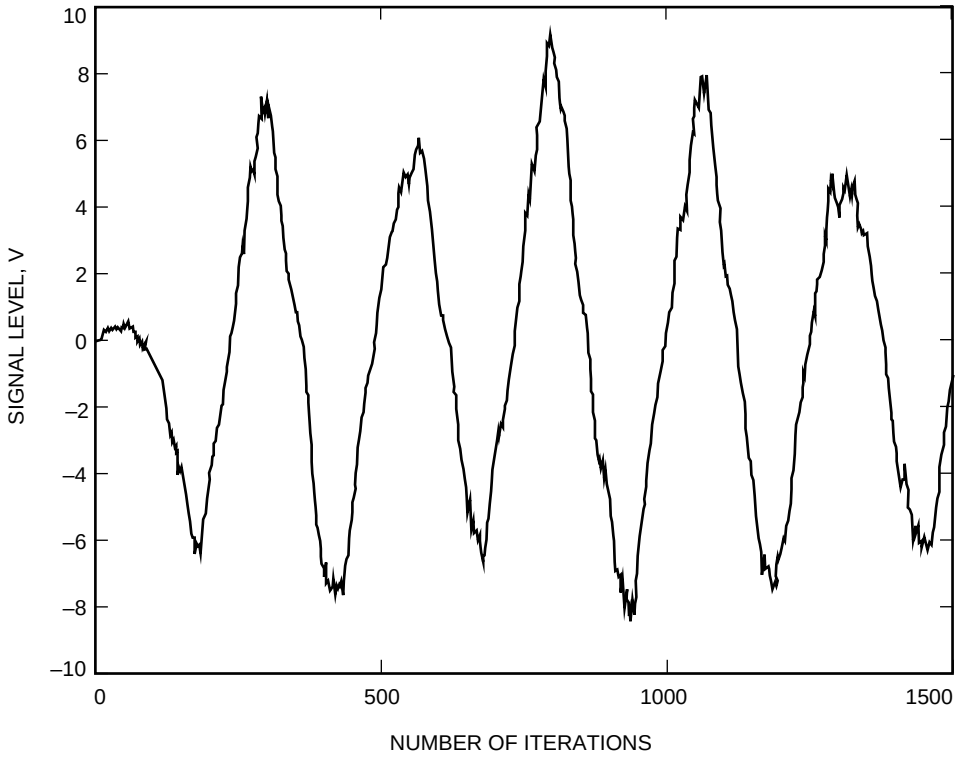

Fig. 13. The 16-tap ALECA output: an estimated carrier signal.

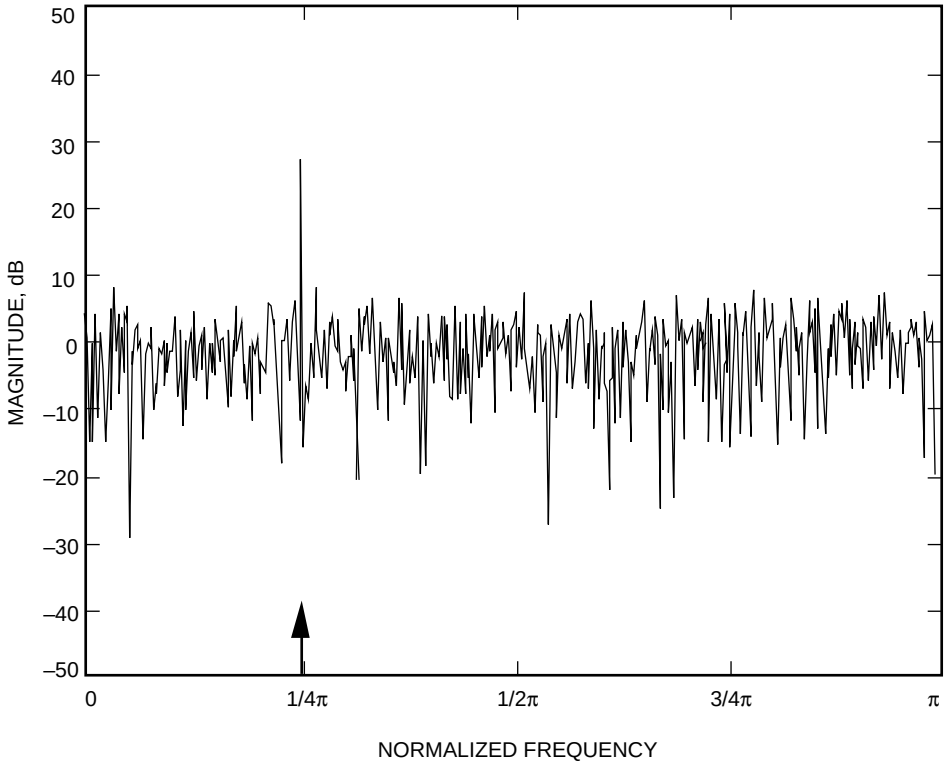

Fig. 14. Magnitude of the input data to the ALE, ALEDF, AND ALECA.

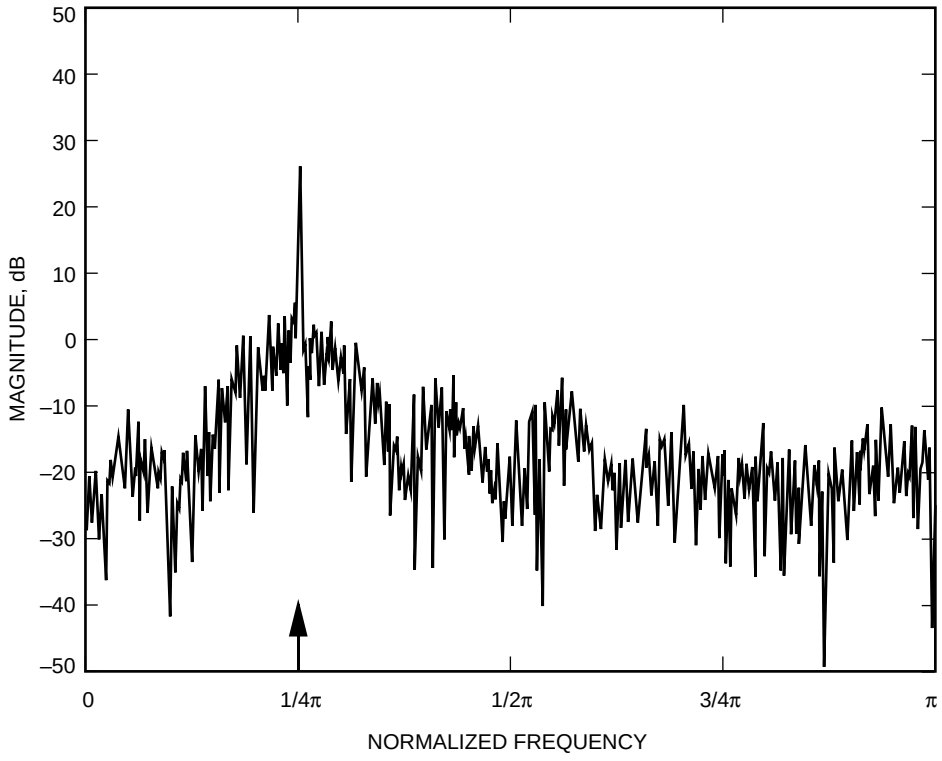

Fig. 15. Magnitude of the ALE output data.

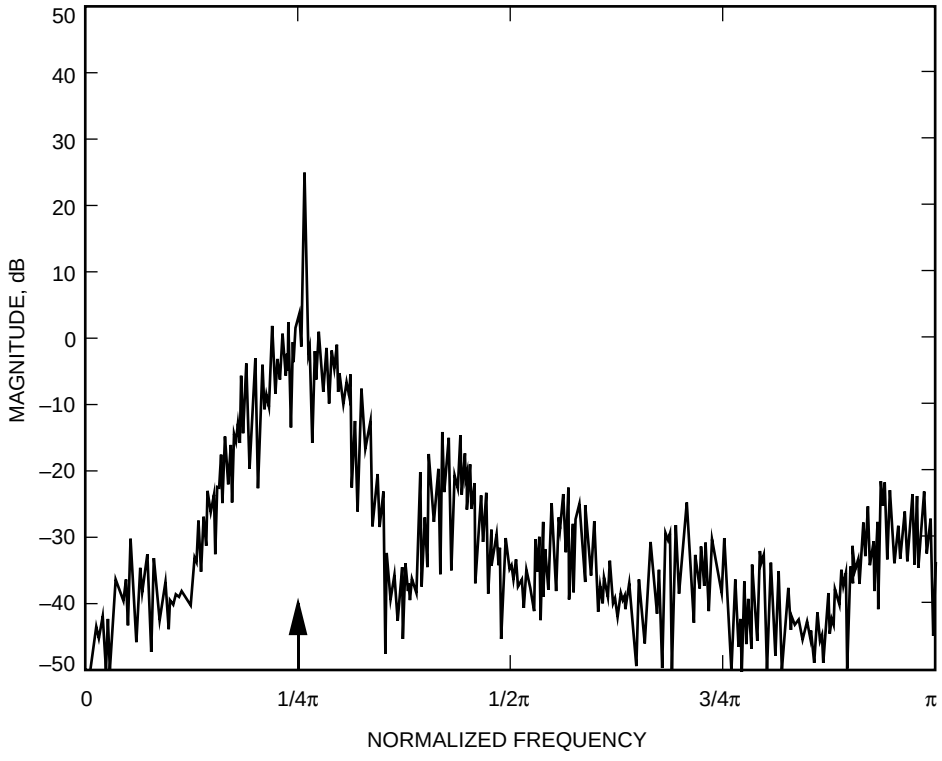

Fig. 16. Magnitude of the ALEDF output data.

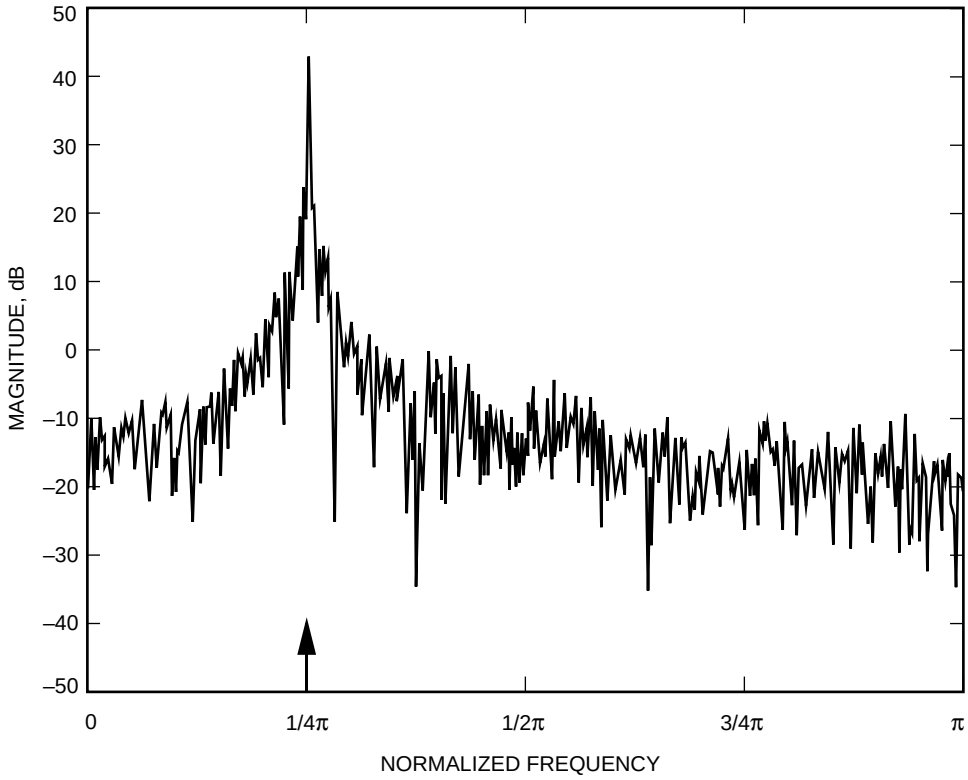

Fig. 17. Magnitude of the ALECA output data.

Furthermore, the ALECA output data provide a very sharp frequency response. These observations all agree with our analysis in Section III.B and as shown in Figs. 6 and 9 for the ALEDF and ALECA, respectively. Theoretically, the SNR of a system using the 16-tap ALE is improved by 12 dB over the same system without the ALE. The performance of both the ALEDF and the ALECA should be better than that of the 16-tap ALE by at most 3 dB, as indicated by Figs. 6 and 9. However, because the weights of these systems slowly fluctuate even in the steady state, the true SNRs at the output are always slightly less than their theoretical values. Note that if the filter length of the ALE is doubled, its theoretical SNR gain becomes 15 dB. However, both the processing time and frequency resolution are doubled.

VI. Discussion and Conclusion

In this article, we presented three ALEs for fast acquisition in the time domain. Conventional ALE, ALEDF, and ALECA systems are introduced. The theoretical performances of these algorithms are presented with computer simulations that support their validity. A fair conclusion is made about both the frequency resolution and processing time.

A. Frequency Resolution

To keep the same frequency resolution, all ALEs have the same number of taps per filter. The positive features of the ALEDF over this conventional ALE are a sharper cutoff frequency in passband and much lower sidelobes in stop band. The advantages of the ALECA over the ALE are a very narrow passband and nearly the same sidelobes in stop band, and a signal gain that can be adjusted by parameter c. The maximum additional CNR gain of either the ALEDF or the ALECA over this conventional ALE is 3 dB due to the second filtering architecture. However, both the ALEDF and the ALECA require 50 percent more computational operations than does the conventional ALE.

B. Processing Time

The filter length of this conventional ALE is twice that of either the ALEDF or the ALECA. Consequently, its frequency resolution is twice that of other ALEs. The advantages of the ALEDF and ALECA over this ALE are a 25-percent saving in multiplications and additions and a 50-percent saving in the memory location required for the weight vector. The CNR gains of both the ALEDF and the ALECA are less than or close to that of this ALE.

These algorithms can be easily implemented via a digital signal processor or application-specific integrated circuits (ASICs) at a sampling frequency of around 100 kHz to acquire the uplink carrier without sweeping the uplink frequency. Furthermore, these algorithms can be easily integrated with either a conventional voltage-controlled oscillator (VCO) in a closed-loop acquisition/tracking architecture, as the present deep-space transponder is, or with a numerically controlled oscillator (NCO) in an open-loop ALE–DFT scheme for acquiring and a closed-loop scheme for tracking the carrier signal.[1]

Acknowledgments

The authors wish to acknowledge the valuable support of Rick Crist and Arthur W. Kermode, and special thanks to Selahattin Kayalar, Sami M. Hinedi, and V. A. Vilnrotter for their careful review, correction, and discussions.

References

[1] S. Acquirre, D. H. Brown, and W. J. Hurd, "Phase Lock Acquisition for Sampled Data PLLs Using the Sweep Technique," *The Telecommunications and Data Acquisition Progress Report 42-86, vol. April–June 1986*, Jet Propulsion Laboratory, Pasadena, California, pp. 95–102, August 15, 1986.

[2] B. Shah and S. Hinedi, "A Comparison of Open-Loop Frequency Acquisition Techniques for Suppressed Carrier Biphase Signals," *The Telecommunications and Data Acquisition Progress Report 42-103, vol. July–September 1990*, Jet Propulsion Laboratory, Pasadena, California, pp. 170–188, November 15, 1990.

[3] M. Aung, W. J. Hurd, C. M. Buu, J. B. Berner, S. A. Stephens, and J. M. Gevargiz, "Block V Receiver Fast Acquisition Algorithm for the Galileo S-band Mission," *The Telecommunications and Data Acquisition Progress Report 42-118, vol. April–June 1994*, Jet Propulsion Laboratory, Pasadena, California, pp. 83–114, August 15, 1994.

[4] R. Kumar, "Fast Frequency Acquisition via Adaptive Least Squares Algorithm," *The Telecommunications and Data Acquisition Progress Report 42-85, vol. January–March 1986*, Jet Propulsion Laboratory, Pasadena, California, pp. 53–61, May 15, 1986.

[1] T. M. Nguyen and H. G. Yeh, "A New Carrier Frequency Acquisition Technique for Future Digital Transponders," in preparation for publication.

[5] B. Widrow, J. R. Tlover, J. M. Cool, J. Kaunitz, C. S. Williams, R. H. Hearn, J. R. Zeidler, E. Dong, Jr., R. C. Goodlin, "Adaptive Noise Canceling Principles and Applications," *Proceedings of the IEEE*, vol. 63, pp. 1692–1716, December 1975.

[6] L. Griffiths, "Rapid Measurement of Digital Instantaneous Frequency," *IEEE Trans. Acoustic, Speech, Signal Processing*, vol. ASSP-23, no. 2, pp. 207–222, April 1975.

[7] J. R. Zeidler and D. M. Chabries, "An Analysis of the LMS Adaptive Filter Used as a Spectral Line Enhancer," Tech. Note 1476, Naval Undersea Center, Alexandria, Virginia, February 1975.

[8] W. S. Burdic, "Detection of Narrow-Band Signals Using Time-Domain Adaptive Filter," *IEEE Trans. Aerosp. Electron. Syst.*, vol. AES-14, pp. 578–591, July 1978.

[9] J. T. Richard, J. R. Zeidler, M. J. Dentino, and M. Shensa, "A Performance Analysis of Adaptive Line Enhancer-Augmented Spectral Detectors," *IEEE Trans. Acoustic, Speech, Signal Processing*, vol. ASSP–29, pp. 694–701, June 1981.

[10] N. J. Bershad, "On the Real and Complex Least Mean Square Adaptive Filter Algorithms," *Proceedings of the IEEE*, vol. 69, no. 4, pp. 469–470, April 1981.

[11] B. T. Ho, "An Improvement of Adaptive Line Enhancer by Means of Coherent Accumulation Algorithm," *Chinese Journal of Acoustics*, vol. 9, no. 4, 1991.

[12] D. W. Tufts, L. J. Griffiths, B. Widrow, J. Glover, J. McCool, and J. Treichler, "Adaptive Line Enhancement and Spectrum Analysis," *Proceedings of the IEEE, Letter*, pp. 169–173, January 1977.

Appendix
Stability of the ALECA

From the transfer function $\mathbf{H}_a(z)$, the pole of the ALECA can be found from the characteristic equation:

$$1 - z_o z^{-1} - c\beta(z_o z^{-1})^m(1 - (z_o z^{-1})^{L+1}) = 0 \tag{A-1}$$

Let $z_o z^{-1} = x$; Eq. (A-1) becomes

$$1 - x - c\beta x^m(1 - x^{L+1}) = 0 \tag{A-2}$$

or

$$\frac{1}{c\beta x^m} = \frac{1 - x^{L+1}}{1 - x} \tag{A-3}$$

Let $x = 1 - \Delta x$ and consider the pole closed to the unit circle (i.e,. $\Delta x \approx 0$); make the Taylor's series expansion of x in Eq. (A-3) and take only the first-order term as the approximation:

$$\frac{1}{c\beta(1 - m\Delta x)} = \frac{1 - (1 - (L+1)\Delta x)}{1 - (1 - \Delta x)} \tag{A-4}$$

Solving for Δx,

$$\Delta x = \frac{(L+1)\beta c - 1}{(L+1)\beta c m} < 0 \qquad \text{if } 0 \le c < 1 \tag{A-5}$$

This implies

$$pole \ = z = \frac{z_o}{1 - \Delta x} \tag{A-6}$$

Since Δx is less than 0 by choosing $0 \le c < 1$ and the magnitude of z_o is equal to 1, the pole is always located inside a unit circle. Consequently, the ALECA is always stable.